

Sequential Neural Posterior and Likelihood Approximation

Samuel Wiqvist¹, Jes Frellsen^{2,*}, Umberto Picchini^{3,*}

¹Centre for Mathematical Sciences, Lund University, Lund, Sweden

²Department of Applied Mathematics and Computer Science, Technical University of Denmark, Denmark

³Department of Mathematical Sciences, Chalmers University of Technology and the University of Gothenburg, Gothenburg, Sweden

Abstract

We introduce the *sequential neural posterior and likelihood approximation* (SNPLA) algorithm. SNPLA is a normalizing flows-based algorithm for inference in implicit models. Thus, SNPLA is a simulation-based inference method that only requires simulations from a generative model. Compared to similar methods, the main advantage of SNPLA is that our method jointly learns both the posterior and the likelihood. SNPLA completely avoids Markov chain Monte Carlo sampling and correction-steps of the parameter proposal function that are introduced in similar methods, but that can be numerically unstable or restrictive. Over four experiments, we show that SNPLA performs competitively when utilizing the same number of model simulations as used in other methods, even though the inference problem for SNPLA is more complex due to the joint learning of posterior and likelihood function.

1 Introduction

Simulation-based inference refers to methods that allow for inference in implicit statistical models, meaning that the likelihood function is only known implicitly via simulations from a generative model. Traditionally, approximate Bayesian computation (ABC) (Beaumont et al., 2002; Marin et al., 2012) is the most popular methodology for inference in implicit models. Other important methods include: synthetic likelihoods (SL) (Wood, 2010; Price et al., 2018), Bayesian optimization (Gutmann & Corander, 2016), classification based methods such as likelihood-free inference by ratio estimation (LFIRE) (Thomas et al., 2020), and pseudomarginal methods (Andrieu & Roberts, 2009; Andrieu et al., 2010). More recently several machine-learning-based methods have also been developed, see Cranmer et al. (2020) for an overview, and some of these methods have been benchmarked in Lueckmann et al. (2021). Normalizing flows (Kobyzev et al., 2020) have also recently been used in simulation-based inference (Papamakarios et al., 2019b; Greenberg et al., 2019; Radev et al., 2020), in particular due to the ease of simulation, and density evaluation (Papamakarios et al., 2019a).

Some of the machine-learning based methods that are relevant for our work are: *sequential neural posterior estimation* (SNPE) (Papamakarios & Murray, 2016; Lueckmann et al., 2017; Greenberg et al., 2019); *sequential neural likelihood estimation* (SNL) (Papamakarios et al., 2019b); *sequential neural ratio estimation* (SNRE) (Hermans et al., 2020; Durkan et al., 2020b), and BayesFlow (Radev et al., 2020). Both SNPE and SNL utilize a sequential scheme and learn the distribution of interest *directly*. SNRE instead utilizes a ratio-estimation scheme somewhat similar to the approach of Thomas et al. (2020). Thus SNRE does not directly learn the distribution of interest but, instead, the likelihood ratio. BayesFlow also directly provides an approximation of the posterior distribution. However, BayesFlow is an amortized method that learns the “global posterior distribution” $p(\theta|x)$ for parameter θ based on a generic dataset x , while SNPE and SNL learn the posterior $p(\theta|x_{\text{obs}})$ for some specific observed data set x_{obs} .

Our work will focus in particular on SNL and SNPE, since our method SNPLA is inspired by both. SNL and SNPE are fairly similar since both utilize a sequential scheme to directly learn the posterior (SNPE) or the likelihood (SNL). The training data is generated from a proposal distribution that is sequentially made more informed, conditionally on the observed data at hand. The posterior models have been expressed using density estimation networks in Papamakarios & Murray (2016); Lueckmann et al. (2017), while recent contributions (Papamakarios et al., 2019b; Greenberg et al., 2019) utilize normalizing flows.

The main disadvantage of SNPE is the *correction step* that must be used so that SNPE learns the correct posterior distribution. SNL avoids this correction step (since SNL learns the likelihood model). However, SNL relies on Markov chain Monte Carlo (MCMC) for sampling from the posterior, which is time-consuming and restricts which posteriors can be learned, since MCMC exploration of complex surfaces (e.g. multi-modal targets) can be challenging. Our SNPLA addresses both these issues by: (i) avoiding the correction step in SNPE by utilizing the reverse Kullback–Leibler (KL) divergence, and (ii) modeling both an approximate posterior and an approximate likelihood via normalizing flows, which allows for efficient sampling from both. The “learned” likelihood model (a normalizing flow model) approximates the data generating process. Thus by sampling from the learned likelihood model, the re-

*Equal contribution.

Contact: samuel.wiqvist@matstat.lu.se; jefr@dtu.dk; picchini@chalmers.se.

Code: <https://github.com/SamuelWiqvist/snpla>.

searcher can rapidly generate artificial data from an approximate generative model. Of course, the latter will be most informative for input parameters that are similar to those that generated the observed data set x_{obs} .

Our **main contribution** is: We introduce SNPLA, a simulation-based inference methods that: (i) avoids the correction step in SNPE; (ii) avoids MCMC-based sampling of posterior draws, unlike SNL; and, (iii) jointly learns an approximation of the likelihood and the posterior, whereas SNPE is not able to learn the likelihood model, and SNL learns it at a high computational cost.

2 Simulation-based inference for implicit models

The implicit statistical model is given by

$$\theta \sim p(\theta), \quad x \sim p(x|\theta),$$

where $p(x|\theta)$ is the likelihood function associated to a generic x , and whose functional form we assume unknown. However, we assume the likelihood to be implicitly encoded via an associated computer *simulator* that allows us to generate artificial data, conditionally on an input given by some arbitrary parameter θ and a stream of pseudorandom numbers (and possibly additional covariates or inputs that we do not explicitly represent in our notation). The parameter prior $p(\theta)$ specifies our a-priori beliefs regarding θ . Implicit models are flexible since they only require us to specify a simulator and not the functional form of the likelihood. The goal of the inference task is typically to learn the parameter posterior $p(\theta|x_{\text{obs}})$ for some observed data set x_{obs} .

As motivated in the Introduction, we are going to focus on SNPE and SNL. SNPE directly learns an approximation $\tilde{p}(\theta|x_{\text{obs}}; \beta_P)$ to the parameter posterior, while SNL learns an approximation $\tilde{p}(x|\theta; \beta_L)$ of the global likelihood. The models are parameterized with the weights β_P and β_L respectively. However, the global likelihood model $\tilde{p}(x|\theta; \beta_L)$ is trained with data influenced by the observed data set x_{obs} . This means that $\tilde{p}(x|\theta; \beta_L)$ will be most accurate for values of θ having high density under the posterior $p(\theta|x_{\text{obs}})$. The models $\tilde{p}(\theta|x; \beta_P)$ and $\tilde{p}(x|\theta; \beta_L)$ can either be conditional density estimators (Papamakarios & Murray, 2016; Lueckmann et al., 2017) or conditional normalizing flows (Papamakarios et al., 2019b; Greenberg et al., 2019; Lueckmann et al., 2017). Both SNPE and SNL start off with simulating training data for the posterior or the likelihood model from a proposal distribution $\hat{p}(\theta|x_{\text{obs}})$ that in the first iteration is set to the prior $p(\theta)$. The proposal distribution is then sequentially adapted to leverage more information from the most recent approximation of the posterior. The overall structure of the SNPE and the SNL schemes is outlined below:

1. Set the proposal $\hat{p}(\theta|x_{\text{obs}})$ to the prior, i.e. $\hat{p}(\theta|x_{\text{obs}}) \equiv p(\theta)$

2. Iterate the following scheme R times, i.e. for $r = 1 : R$ do:

- i. Sample $\theta_n \sim \hat{p}(\theta|x_{\text{obs}})$, for $n = 1 : N$;
- ii. Generate $x_n \sim p(x|\theta_n)$, for $n = 1 : N$;
- iii. **For SNL:** (Re)-train the likelihood model $\tilde{p}(x|\theta)$ using the samples $[\theta_{1:N}, x_{1:N}] \cup \{\text{all samples from previous iterations}\}$. The likelihood model is updated by maximizing $\log \tilde{p}(x|\theta; \beta_L)$ with respect to β_L , which corresponds to minimizing the following loss:
$$\mathcal{L}(\beta_L) = -E_{\tilde{p}(\theta, x) = p(x|\theta)\hat{p}(\theta|x_{\text{obs}})}(\log \tilde{p}(x|\theta; \beta_L)).$$
- iv. **For SNL:** Update the proposal distribution, i.e. set

$$\hat{p}(\theta|x_{\text{obs}}) \propto \tilde{p}(x_{\text{obs}}|\theta; \beta_L)p(\theta).$$

- iii'. **For SNPE:** (Re)-train the posterior model $\tilde{p}(\theta|x)$ using the samples $[\theta_{1:N}, x_{1:N}] \cup \{\text{all samples from previous iterations}\}$. The posterior model is updated by maximizing $\log \tilde{p}(\theta|x; \beta_P)$ with respect to β_P , which corresponds to minimizing the following loss:

$$\mathcal{L}(\beta_P) = -E_{\tilde{p}(\theta, x) = p(x|\theta)\hat{p}(\theta|x_{\text{obs}})}(\log \tilde{p}(\theta|x; \beta_P)).$$

- iv'. **For SNPE:** Update the proposal distribution, i.e. set

$$\hat{p}(\theta|x_{\text{obs}}) \leftarrow \frac{p(\theta)}{\hat{p}(\theta|x_{\text{obs}})} \tilde{p}(\theta|x_{\text{obs}}; \beta_P).$$

In step 2iv', we see that the updated proposal distribution for SNPE is corrected with the factor $p(\theta)/\hat{p}(\theta|x_{\text{obs}})$. This *correction step* is necessary to ensure that the newly constructed parameter proposal is valid, see Papamakarios & Murray (2016) for details. The correction step can either be done analytically (Papamakarios & Murray, 2016), numerically (Lueckmann et al., 2017), or via reparameterization (Greenberg et al., 2019). An intuitive explanation is the following: this correction can be viewed as an ‘‘importance weighting’’ step that is necessary since we are updating the posterior model with data generated from the proposal distribution instead of the prior. The correction step can introduce complexities into SNPE. For example, the closed-form correction of Papamakarios & Murray (2016) can be numerically unstable (if the proposal prior has higher precision than the estimated conditional density) and is restricted to Gaussian and uniform proposals, limiting both the robustness and flexibility of the approach. Regarding the correction in Lueckmann et al. (2017), the introduction of importance weights greatly increases the variance of parameter updates during learning, which can lead to slow or inaccurate inference (Greenberg et al., 2019). For SNL this correction is not necessary since SNL learns the likelihood model $\tilde{p}(x|\theta; \beta_L)$. On the other hand, SNL uses MCMC sampling in step 2i, which is time-consuming and unfeasible for some targets with complex geometries.

2.1 Normalizing flows for simulation-based inference

Since our proposed method uses normalizing flows, here we introduce some basic notions. The normalizing flow model, introduced in Rezende & Mohamed (2015) (see Kobyzev et al., 2020; Papamakarios et al., 2019a for reviews), is a probabilistic model that transforms a simple *base distribution* $u \sim p_u(u)$ into some complex distribution $x \sim p_x(x)$ via the following transformation

$$x = T(u), \quad u \sim p_u(u).$$

The function T is parameterized with an *invariant* neural network such that T^{-1} exists, and that both T and T^{-1} are differentiable, i.e. the function T is *diffeomorphic*. The probability density function (pdf) for x is computed via the Jacobian J_T of T (or $J_{T^{-1}}$ of T^{-1}) in the following two equivalent ways:

$$\begin{cases} p(x) &= p_u(u) |\det J_T(u)|^{-1}, & u \sim T^{-1}(x), \\ p(x) &= p_u(T^{-1}(x)) |\det J_{T^{-1}}(x)|. \end{cases}$$

Due to this structure of the pdf, it is easy to construct complex transformations by composing, say, n transformations such that $T = T_1 \circ T_2 \circ \dots \circ T_n$ where each transformation T_i is diffeomorphic, and where the Jacobian contribution for each T_i can be computed. Flow models that allow for building these kinds of nested structures are, for instance, RNVP (Dinh et al., 2017), Neural Spline Flow (Durkan et al., 2019), and Masked Autoregressive Flow (Papamakarios et al., 2017). Now, assume that we have a normalizing flow model $\tilde{p}_x(x; \beta)$ (with weights β for neural network T), and that our target distribution is denoted $p_x(x)$. We want to train $\tilde{p}_x(x; \beta)$ so that it approximates $p_x(x)$. Let us also assume that we can obtain samples from the target $p_x(x)$, then we can use the *forward* KL divergence to fit the flow model by utilizing the following loss function

$$\begin{aligned} \mathcal{L}(\beta) &= D_{KL}[p_x(x) \parallel \tilde{p}_x(x; \beta)], \\ &= -E_{p_x(x)}[\tilde{p}_x(x; \beta)] + \text{const.}, \\ &= -E_{p_x(x)}[\log p_u(T^{-1}(x; \theta))] + \\ &\quad \log |\det J_{T^{-1}}(x; \beta)| + \text{const.} \end{aligned} \quad (1)$$

The loss in (1) is typically (and also in our case) evaluated via Monte Carlo.

If we do not have access to samples from the target distribution $p_x(x)$, but we can evaluate the pdf of $p_x(x)$, it is possible to fit $\tilde{p}_x(x; \beta)$ via the *reverse* KL divergence using the loss

$$\begin{aligned} \mathcal{L}(\beta) &= D_{KL}[\tilde{p}_x(x; \beta) \parallel p_x(x)], \\ &= -E_{\tilde{p}_x(x; \beta)}[\tilde{p}_x(x; \beta) - \log p_x(x)] + \text{const.}, \\ &= -E_{\tilde{p}_x(x; \beta)}[\log p_u(u)] + \\ &\quad \log |\det J_T(u; \beta)| - \log p_x(T(u; \beta)) + \text{const.} \end{aligned}$$

It is shown in Papamakarios et al. (2017) that the forward and the reverse KL divergence are equivalent. The possibility to fit the flow model $\tilde{p}_x(x; \beta)$ via the

reverse KL divergence is critical for our method, since SNPLA uses it to train the posterior model without using a proposal distribution, more on this is in Section 3.

Normalizing flows have been used for simulation-based inference in several papers (Radev et al., 2020; Papamakarios et al., 2019b; Greenberg et al., 2019), either for modeling the likelihood or the posterior. Using normalizing flows for simulation-based inference is also particularly fruitful since both sampling and density estimation can be done efficiently (Papamakarios et al., 2019a).

3 Sequential neural posterior and likelihood approximation

Here we detail our proposed method. The main idea of the SNPLA method is to jointly learn both an approximation of the parameter posterior $\tilde{p}(\theta|x_{\text{obs}}; \beta_P)$, and an approximation of the likelihood $\tilde{p}(x|\theta; \beta_L)$. Thus SNPLA has two learnable models:

1. **Parameter posterior model** $\tilde{p}(\theta|x_{\text{obs}}; \beta_P)$, approximating the parameter posterior distribution $p(\theta|x_{\text{obs}})$.
2. **Likelihood model** $\tilde{p}(x|\theta; \beta_L)$. Since we are considering an implicit statistical model, we consider the likelihood model $\tilde{p}(x|\theta; \beta_L)$ as approximating the data generating process $p(x|\theta)$.

Both the posterior model and the likelihood model are parameterized via normalizing flows, with weights β_P and β_L respectively. The use of normalizing flows is also critical since these can be trained using either the forward or the reverse KL divergence.

For SNPLA the likelihood model $\tilde{p}(x|\theta; \beta_L)$ is learned via training data sampled from a proposal distribution $\tilde{p}(\theta|x_{\text{obs}})$. However, the obtained likelihood approximation $\tilde{p}(x|\theta; \beta_L)$ is also used to train the posterior model $\tilde{p}(\theta|x_{\text{obs}}; \beta_P)$, so that we jointly learn both the posterior and the likelihood. The SNPLA scheme at iteration $r = 1 : R$ is outlined below:

1. **Update the likelihood model** with training data sampled from a mixture of the prior and the current posterior model:

- i. Sample for $n = 1 : N$

$$\theta_n \sim \hat{p}(\theta|x_{\text{obs}}) = \alpha p(\theta) + (1 - \alpha) \tilde{p}(\theta|x_{\text{obs}}; \beta_P),$$

where, for example, $\alpha = \exp(-\lambda \cdot (r - 1))$ with $\lambda > 0$;

- ii. Generate $x_n \sim p(x|\theta_n)$, for $n = 1 : N$;
- iii. Update $\tilde{p}(x|\theta; \beta_L)$ using the samples $[\theta_{1:N}, x_{1:N}]$ from the mixture prior-predictive distribution $\hat{p}(\theta, x|x_{\text{obs}}) \propto p(x|\theta) \hat{p}(\theta|x_{\text{obs}})$, with the loss:

$$\begin{aligned} \mathcal{L}(\beta_L) &= D_{KL}(p(x|\theta)) \parallel \tilde{p}(x|\theta; \beta_L) \\ &\propto -E_{\hat{p}(\theta, x|x_{\text{obs}})}[\log \tilde{p}(x|\theta; \beta_L)]. \end{aligned}$$

- 2'. **Hot-start for learning the posterior model (this step only applies to iteration $r = 1$).** We update the posterior model using the prior-predictive samples $[\theta_{1:N}, x_{1:N}]$ generated in step 1. The posterior model is updated with the following loss:

$$\mathcal{L}(\beta_P) \propto -E_{p(\theta, x)=p(x|\theta)p(\theta)} [\log \tilde{p}(\theta|x; \beta_P)].$$

2. **Update the posterior model.** We update the posterior model using training data generated from the current posterior model: Loop over the number of mini-batches N_P/N_{mini} , i.e. for $j = 1 : N_P/N_{\text{mini}}$:

- i. For $i = 1 : N_{\text{mini}}$: Sample $\theta_i \sim \tilde{p}(\theta|x_{\text{obs}}; \beta_P)$;
- ii. Update posterior model, i.e. minimize the loss (reverse KL divergence):

$$\mathcal{L}(\beta_P) = D_{KL}(\tilde{p}(\theta|x_{\text{obs}}; \beta_P) || \tilde{p}(x_{\text{obs}}|\theta; \beta_L)p(\theta))$$

In step 1, as the iteration counter r increases, the mixture probability α exponentially decreases and fewer and fewer samples are proposed from the prior (notice that a different decreasing schedule can be selected for α), hence the likelihood model $\tilde{p}(x|\theta; \beta_L)$ is updated with data generated via the proposal distribution $\hat{p}(\theta|x_{\text{obs}})$, where the latter is set to sequentially leverage more information from the posterior model $\tilde{p}(\theta|x_{\text{obs}}; \beta_P)$. The parameter λ governs how rapidly we want to leverage information from the posterior model. In practice, we have found it useful to use a rather high $\lambda \approx 0.7 - 0.9$, so that the proposal distribution is quickly adapted. N governs the number of training data points used in this step. However, since we need to run N model simulation in step 1 it is advantageous to keep N conservative, particularly if the model simulator is slow. In step 2' the posterior model is updated with samples from the prior-predictive distribution. This step is included on pragmatic grounds since we found SNPLA to exhibit convergence problems if this step is not included. The convergence problems appeared in the first iteration of the algorithm and were probably related to trying to fit the very flexible untrained posterior model $\tilde{p}(\theta|x_{\text{obs}}; \beta_P)$ to a target based on the likelihood model $\tilde{p}(x|\theta; \beta_L)$ obtained after only one iteration of the algorithm (thus, in this iteration, the target for the posterior model itself will be quite uninformative of the actual posterior distribution, which made it hard to fit the posterior model $\tilde{p}(\theta|x_{\text{obs}}; \beta_P)$). Step 2' therefore acts as a pre-training step of the posterior model $\tilde{p}(\theta|x_{\text{obs}}; \beta_P)$. Finally, in step 2, the posterior model is updated with samples generated from the current version of the posterior model. These samples are generated via a *simulation-on-fly* scheme where each mini-batch is simulated from the most recent version of the posterior model. This means that in step 2 we loop over the number of mini-batches N_P/N_{mini} (N_{mini} being the number of samples in one mini-batch, and N_P the total number of samples), and for each mini-batch we simulate new training data. Thus, each mini-batch used in step 2 is unique, since

it is simulated from the most recent posterior approximation. Since in step 2 training data is generated from the flow model, we can take N_P to be much larger than N , and typically one order of magnitude larger. We also see that the current likelihood model is used to set the posterior model's target distribution. Thus in SNPLA the data is used to update the likelihood model partially generated from the current posterior model, and the posterior model is set to approximate the posterior distribution induced by the current version of the likelihood model. Due to this nested and sequential learning approach, SNPLA can exhibit convergence problems if the learning of the likelihood or the posterior model is not appropriately initialized. As previously mentioned, we have found the hot-start approach in step 2' to alleviate these problems. The losses in step 1 and step 2ii are approximated via Monte Carlo, and are learnt via stochastic gradient descent (using the Adam optimizer, Kingma & Ba (2014)). We have found that SNPLA can be sensitive to the learn-rate used for the posterior model. We have obtained the best results when using a moderate to large learn-rate for the posterior model during the first few iterations, which is then sequentially decreased. This allows the posterior model to rapidly explore the weights space in the early iterations and find a reasonable approximation to the posterior. When decreasing the learn-rate, we avoid large catastrophic moves of the posterior model's weights which gets fine-tuned thanks to the access to more data.

3.1 Learning summary statistics

So far, we denoted with $\tilde{p}(\theta|x_{\text{obs}})$ the posterior model that SNPLA learns. However, we can also condition on some function $S(\cdot)$ of the data. In that case, we obtain the following model

$$\tilde{p}(\theta|S(x_{\text{obs}}; \beta_{P_S}); \beta_P). \quad (2)$$

where β_{P_S} denotes weights that are specific for function $S(\cdot)$, since in our work we assume $S(\cdot)$ parameterized with some neural network. We can interpret the function $S(\cdot)$ as mapping the data x_{obs} into a set of summary statistics of the data $S(x_{\text{obs}})$. Considering (2) can be particularly useful if x_{obs} is high-dimensional and/or contains some spatial or temporal structure. Thus we want the network $S(\cdot; \beta_{P_S})$ to leverage the features of the data x_{obs} and therefore, for exchangeable data, we could for instance use a DeepSets network (Zaheer et al., 2017), and for Markovian time-series data it is possible to use a partially exchangeable network (Wiqvist et al., 2019). The network $S(\cdot; \beta_{P_S})$ is trained jointly with the posterior model in (2). So, when incorporating trainable summary statistics, step 2 of SNPLA is modified so that the posterior model and the summary statistics network are updated according to the following loss

$$\mathcal{L}(\beta_P, \beta_{P_S}) = D_{KL}(\tilde{p}(\theta|S(x_{\text{obs}}; \beta_{P_S}); \beta_P) || \tilde{p}(x_{\text{obs}}|\theta; \beta_L)p(\theta)).$$

Importantly, notice that the summary statistics network $S(\cdot; \beta_{P_S})$ is not included in the likelihood model $\tilde{p}(x|\theta; \beta_L)$. The likelihood model still learns a model of the full data set x_{obs} , and not a model for the set of summary statistics computed by $S(\cdot; \beta_{P_S})$. However, for complex data with spatial or temporal structures $\tilde{p}(x_{\text{obs}}|\theta; \beta_L)$ can be set-up so that these data features are leveraged in the likelihood model. For instance, specialized flow models for images, audio, and text data have been developed (Papamakarios et al., 2019a), and these can be used in the likelihood model to leverage the data features.

4 Experiments

We consider the following case-studies: a multivariate (MV) Gaussian model, the two-moons model (Greenberg et al., 2019), the Lotka-Volterra (LV) model, and the Hodgkin-Huxley (HH) model. For all experiments, except the HH model, we compare the following inference methods: SMC-ABC (Beaumont et al., 2009), SNL (Papamakarios et al., 2019b), SNPE-C (Greenberg et al., 2019), SNPR-B (Durkan et al., 2020b), and SNPLA. For HH we only compare SNL, SNPE-C and SNPLA. However, since SNPLA has strong connections to SNPE-C and SNL, special interest is placed on their comparison. The experiments are set-up so that all methods have access to the same number of model simulations. The normalizing flow models used by SNL, SNPE-C, and SNPLA were set to be the same. The masked autoregressive flow architecture (Papamakarios et al., 2017) was used to construct the flow models. We are primarily interested in comparing the quality of the posterior parameter inference for the different methods. However, we also compare the quality of the likelihood approximation that we obtain from SNL and SNPLA.

The code for replicating the experiments can be found at <https://github.com/SamuelWiqvist/snpla>. Additional technical information and inference results can be found as supplementary material. The most important hyper-parameter settings are also presented in the supplementary material.

4.1 Proof-of-concept: Multivariate Gaussian

We consider the following conjugate MV Gaussian example from Radev et al. (2020)

$$\mu \sim N(\mu|\mu_\mu, \Sigma_\mu), \quad x \sim N(x|\mu, \Sigma),$$

where both Gaussians have dimension two. The covariance Σ is assumed to be known, so the main goal here is to infer the posterior for the mean $p(\mu|x_{\text{obs}})$. The posterior $p(\mu|x_{\text{obs}})$ is analytically known and we evaluate the quality of the inference by computing the KL divergence between the analytical and the approximate posterior, for details see the supplementary material.

We consider three versions of the MV Gaussian study: (i) “five observations”, where data x_{obs} consists of five two-dimensional samples, and the likelihood model

$\tilde{p}(x|\theta; \beta_L)$ is set to directly target these five observations; (ii) “summary statistics” where data are given by five summary statistics (the two sample means of the data, the two sample variances and the sample covariance between the two components, i.e. the sufficient statistics for the model) obtained from a two-dimensional vector of 100 observations, and the likelihood model is set to target the summary statistics of these data; and finally (iii) “learnable summary statistics”, where we use a small DeepSets network (Zaheer et al., 2017) to compute the summary statistics following the method in Section 3.1 based on five observations. We ran all methods independently for 10 times (each time with a different set of observed data), using $R = 10$ iterations with $N = 2,500$ model simulations for each iteration. For SNPLA we used $N_P = 10,000$ (recall, N_P is not the number of model simulations. This is just the number of posterior samples from the flow model). For SMC-ABC, however, we utilized up to, in total, $N = 10^6$ model simulations.

Posterior inference for the three versions of the MV Gaussian model is in Figures 1(a), 1(b), and 1(c) (samples from the resulting posteriors are presented as supplementary material). We conclude that all methods, except SMC-ABC, perform similarly well for “five observations”. For “learnable summary statistics” we have that SNPLA is converging slightly worse compared to SNL, SNPE-C, and SNRE-B. For “summary statistics” SNPE-C performs the best, followed by SNL and SNPLA which perform similarly well. Instead, both SMC-ABC and SNRE-B under-perform for the given numbers of model simulations. For “summary statistics” we also check the performance of the likelihood model in SNL and SNPLA by sampling from the approximate posterior predictive distribution obtained from the learned likelihood models. That is, we sampled summary statistics for 1,000 times from $\tilde{p}(x|\theta; \beta_L)$, where β_L is the one returned at iteration R and conditionally on posterior draws of θ from the analytical posterior distribution. These results are presented in Figure 2, and we conclude that SNL and SNPLA perform similarly well. The samples from the approximate posterior predictive distributions also match well with the samples from the analytical posterior predictive. Notice that a comparison like the one in Figure 2 is not possible with SNPE-C, since the latter would need access to the true model simulator, while with SNPLA (and SNL) we can make use of a learned likelihood model, i.e. a cheap simulator. This ability is particularly relevant when the true simulator is computationally expensive.

4.2 Complex posterior: Two-moons

The two-moons (TM) example (Greenberg et al., 2019) is a more complex static model. An interesting feature is that the posterior, in some cases, is crescent-shaped. For a technical description of the model, see the supplementary material.

We ran all methods 10 times (each time with the same observed data set) for $R = 5$ iterations and using $N = 2,000$ model simulations for each iteration, and

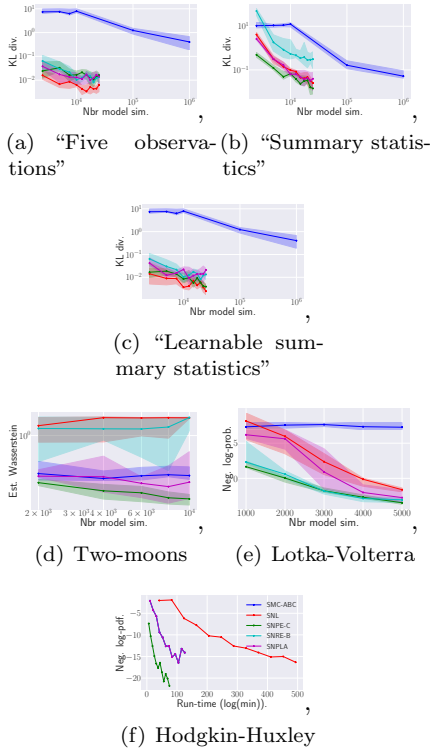


Figure 1: MV:Gaussian/Two-moons/Lotka-Volterra/Hodgkin-Huxley: Posterior inference results for “five observations”, “summary statistics”, “learnable summary statistics”, Two-moons, Lotka-Volterra, and Hodgkin-Huxley. SMC-ABC results (blue); SNL (red); SNPE-C (green); SNRE-B (cyan); SNPLA (magenta). The solid lines show the median value over the attempts and the shaded areas show the range for the 25th and 75th percentile. The results for Hodgkin-Huxley are based on one run of each method and each marker indicates one iteration using 2,000 model simulations.

for SNPLA $N_P = 40,000$ samples. We evaluate the posterior accuracy via the Wasserstein distance between the analytical posterior and the approximate posteriors. The mathematical definition of the Wasserstein distance, and information on how it is computed, are provided in the supplementary material.

Inference results are in Figures 1(d) and 3. We conclude that SNPE-C performs the best. SNPLA also performs well, in particular in many cases the distances from SNPLA are smaller than those from SMC-ABC, however the variability in performance for SNPLA is larger. Indeed while SMC-ABC manages to “visit” both crescent moons, the extent of the exploration for each moon is quite poor (it is only a consequence of the method’s construction that makes it appear as in Figure 3 this has fewer samples than expected; actually many of those overlap on top of each-other). Finally, SNL and SNRE-B perform significantly worse than the other methods. SNL and SNRE-B presumably do not perform well here since both use an MCMC sampler, which can struggle to efficiently explore the

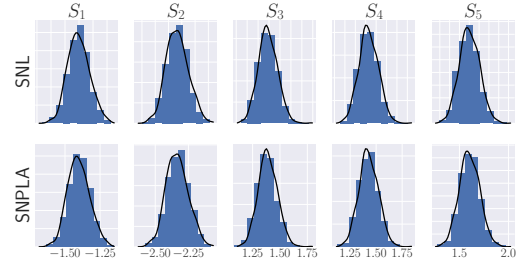


Figure 2: MV Gaussian (“summary statistics”): Marginal normalized histograms of the samples from the resulting posterior predictive distribution, i.e samples from the learned likelihood model, conditionally on parameters θ from the true posterior. The black lines are smoothed marginal densities of samples from the true likelihood model.

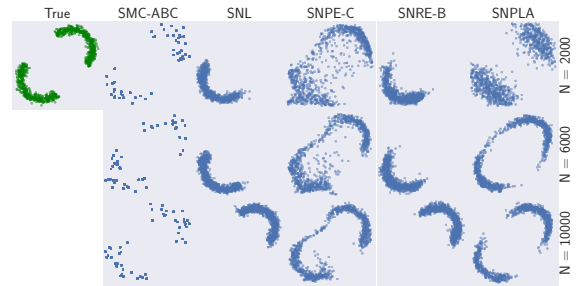


Figure 3: TM: Samples from the approximate posterior distributions and the exact one. Results from one of the ten runs. Results from the first iteration (top), from the third iteration (middle) and the fifth iteration (bottom).

bimodal target. These results are in line with those in Greenberg et al. (2019). We also compare the approximate likelihood models that we learned via SNL and SNPLA. To this end, we simulated data from the learned likelihood models at parameter values simulated from the true posterior. To investigate the performance of the likelihood models we compute the estimated Wasserstein distance between samples from the analytical likelihood and the likelihood models of SNL and SNPLA. The median and quantiles (Q_{25}, Q_{75}) of the distances follow: SNL: 0.122, (0.133, 0.127), SNPLA: 0.11, (0.107, 0.119). Thus, we again conclude that the likelihood models from SNL and SNPLA perform very similarly.

4.3 Time-series with summary statistics: Lotka-Volterra

Here, we consider the Lotka-Volterra (LV) case study from Papamakarios et al. (2019b). Observations are assumed to be a set of 9 summary statistics computed from the 2-dimensional time-series (for details, see the supplementary material). We ran all methods 10 times (each time with the same observed data set) for $R = 5$

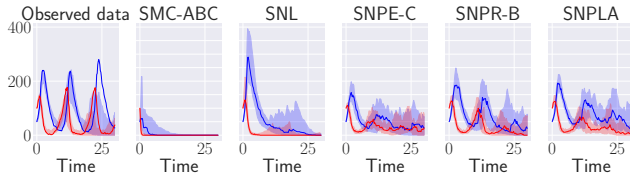


Figure 4: LV: Posterior predictive simulations. The solid lines show the median value over the attempts and the shaded areas show the range for the 25th and 75th percentile.

iterations each using $N = 1,000$ model simulations, and for SNPLA $N_P = 10,000$ samples. We followed Papamakarios et al. (2019b) and evaluated the obtained posterior distribution by computing its negative log-pdf at the ground-truth parameters (for details, see the supplementary material).

Results are in Figure 1(e) (samples from the resulting posterior distributions are presented in the supplementary material). For a large number of model simulations, SNPE-C, SNRA-B, and SNPLA perform similarly well. However, for $N < 4,000$ SNPLA is less precise than SNPE-C and SNRA-B, but performs uniformly better than SNL. Once more, we remind the reader that SNPLA has a more complex task to perform: learning the likelihood and the posterior.

We also ran posterior predictive simulations, that is we simulated from the *true* model conditionally on the obtained parameter posterior draws. See Figure 4 for an example. Simulations from SMC-ABC and SNL do not correspond well with the observed data. However, for SNPE-C, SNPR-B, and SNPLA we observe a more realistic behaviour. The high variability in the model simulations for all methods is due to the intrinsic stochasticity of the LV model.

4.4 Neuronal model: Hodgkin-Huxley model

We now consider the Hodgkin-Huxley (HH) model from Lueckmann et al. (2017); Papamakarios et al. (2019b). The HH model (Hodgkin & Huxley, 1952) is used in neuroscience to model the dynamics of a neuron’s membrane potential as a function of some stimulus (injected current) and a set of parameters. The likelihood $p(x|\theta)$ is defined on 19 summary statistics computed from simulated voltage time-series. Further details about the model can be found in the supplementary material.

For our simulation-study, we have 10 unknown parameters, and the observed data set (see the top left plot in Figure 5) is generated by simulating the model for 200 ms with step-length 0.025 ms. We used SNPE-C, SNL and SNPLA to infer the 10 parameters, and each method has access to $N = 2,000$ model simulations for each of $R = 12$ iterations. Due to the high computational cost of running the methods (in particular SNL), we only ran each method once. For SNPLA, we used $N_P = 10,000$ samples for each iteration. For each

method, the quality of the posterior inference was evaluated by computing the corresponding (approximate) negative log-pdf of the posterior at the ground-truth parameter. We also investigate the quality of the posterior approximation by running posterior predictive simulations, which are obtained by sampling parameter values from the resulting posterior approximation, and then running the HH model simulator at these parameter values.

Posterior inference from using the same number of model simulations is in Figure 1(f). From Figure 1(f) we note that, in terms of the negative log-pdf of the posterior evaluated at the ground truth parameters and for the same number of model simulations, SNL performs marginally better than SNPLA, however, SNPLA converges much faster than SNL in terms of wall-clock time. For instance, obtaining a negative log-pdf value of -15 takes 94 minutes for SNPLA, while SNL obtains the same accuracy in 340 minutes. Samples from the resulting posterior approximations are presented in the supplementary material, and these show that SNPE-C performs better than SNL and SNPLA, while SNL and SNPLA perform similarly well. Also, the approximate marginals overall resemble the inference results presented in Papamakarios et al. (2019b) and Lueckmann et al. (2017), with the exception of the σ parameter, which could be due to the somewhat different experimental setting we use. Posterior predictive simulations in Figure 5 (from using the same number of model simulations) show that SNPE-C and SNPLA perform the same and, to a greater extent, resemble the observed data, while SNL is somewhat slightly worse.

Our conclusion is that SNPE-C learns a somewhat more informative posterior model compared to SNL and SNPLA. We likely obtain these results since the posterior distribution in the HH model is easier to learn than the likelihood. Our conjecture is based on noting that the parameters prior is set to a 10-dimensional uniform distribution, and hence the posterior will have zero mass outside the prior’s bounds and such restrictions are utilized in the flow posterior model (for technical details on this fact, see the supplementary material). However, similar restrictions for the likelihood model cannot be deduced, making it harder to learn the latter. It is also likely that the high variability of the summary statistics makes learning the likelihood challenging.

5 Discussion

We have introduced the SNPLA algorithm. In four case studies, we have shown that SNPLA produces similar posterior inference as other simulation-based algorithms when all methods have access to the same number of model simulations. This is a rather interesting finding since the learning task for SNPLA is more complex compared to the other methods that we compare with, given that SNPLA is set to learn both the posterior model and the likelihood model, whereas SNL and SNPE-C only learn either the likelihood (SNL) or the posterior (SNPE-C). However, the variability of the

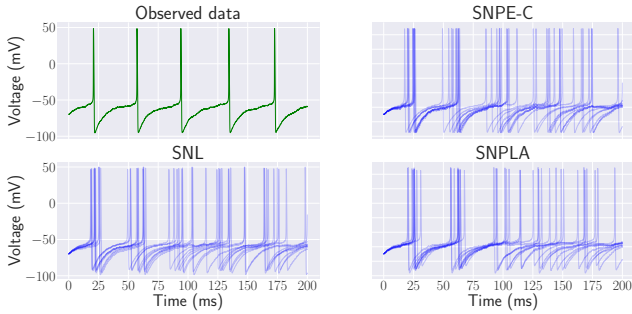


Figure 5: HH: Posterior predictive paths.

inference results obtained with SNPLA is consistently higher, which suggests that SNPLA would need to access more model simulation to obtain inference results *at par* with SNL and SNPE-C. Considering SNPLA’s complex learning task that would, however, not be surprising. For the HH model, we have also shown that SNPLA can converge faster than SNL in terms of wall-clock time.

While comparing run-times has not been the focus of this work, it is indeed the case that SNPLA generates posterior samples much more efficiently than SNL and SNRE-B, since draws from SNPLA are generated by a forward pass of a normalizing flow network, while those from SNL and SNRE-B are generated via MCMC. For instance, for the LV model we have that SNL requires 2,586 seconds to generate 1,000 samples from the approximate posterior distribution, while SNPLA only requires 0.05 seconds for the same number of draws. For the case studies “MV Gaussian model - summary stats” and “Two-moons” the likelihood model learned by SNPLA is also shown to perform similarly well as the likelihood model learned by SNL.

Recently, for simulation-based methods, it has been discussed (Durkan et al., 2018) if it is of advantage to learn the likelihood or the posterior. With this work we show that this question can be circumvented by learning both. An advantage with learning both is that we obtain an approximation of the distribution that is typically of interest, i.e. the posterior, and also obtain an approximate model simulator via the learned likelihood model. Since the latter is a normalizing flows, this opens the possibility for the rapid simulation of artificial data, when the “true simulator” $p(x|\theta)$ cannot be used more than a handful of times due to e.g. financial or computational constraints. We can therefore think of the learned likelihood model $\tilde{p}(x|\theta; \beta_L)$ provided by SNPLA as a “surrogate of the likelihood”, i.e. an approximate simulator. For example, the researcher may be interested in rapidly screening the output of such simulator, for many different parameter values, especially those that have not already been explored during the execution of SNPLA. This can be of interest even when the learned likelihood is defined on summary statistics. As an example: suppose we wish to rapidly screen the parameter space for the HH model to find parameters corresponding to trajectories having

five spikes. If the number of spikes is one of the summaries considered by the learned likelihood, then we can rapidly disregard parameters for which $\tilde{p}(x|\theta; \beta_L)$ outputs a different number of spikes. In other contexts, we could use the surrogate likelihood to estimate tail probabilities for rare events via (otherwise expensive) Monte Carlo simulations. Of course the uncertainty on the approximate simulator’s output will be larger when imputed parameters are very different from those learned from the actual data.

The main drawback of SNPLA is that the algorithm can require several pilot-runs to find a suitable λ and a decrease schedule for the learning rate of the posterior model. Our suggestion is to set λ fairly large ($\lambda \approx 0.7 - 0.9$) so that we rapidly leverage the posterior model, and to set the initial learn-rate rather high and then rapidly decrease it. However, once suitable hyperparameter settings are found, SNPLA learns both the posterior and the likelihood without relying on MCMC sampling or post-hoc correction steps.

Acknowledgements

The computations were enabled by resources provided by the Swedish National Infrastructure for Computing (SNIC) at LUNARC partially funded by the Swedish Research Council through grant agreement no. 2018-05973. We would also like to thank the developers of the following Python packages for providing the software tools used in this paper: `sbi` (Tejero-Cantero et al., 2020), `nflows` (Durkan et al., 2020a), `PyTorch` (Paszke et al., 2019), and `POT: Python Optimal Transport` (Flamary & Courty, 2017). UP acknowledges support from the Swedish Research Council (Vetenskapsrådet 2019-03924) and the Chalmers AI Research Centre (CHAIR).

References

- Andrieu, C. and Roberts, G. O. The pseudo-marginal approach for efficient Monte Carlo computations. The Annals of Statistics, 37:697–725, 2009.
- Andrieu, C., Doucet, A., and Holenstein, R. Particle Markov chain Monte Carlo methods. Journal of the Royal Statistical Society: Series B (Statistical Methodology), 72(3):269–342, 2010.
- Beaumont, M. A., Zhang, W., and Balding, D. J. Approximate bayesian computation in population genetics. Genetics, 162(4):2025–2035, 2002.
- Beaumont, M. A., Cornuet, J.-M., Marin, J.-M., and Robert, C. P. Adaptive approximate bayesian computation. Biometrika, 96(4):983–990, 2009.
- Carnevale, N. T. and Hines, M. L. The NEURON book. Cambridge University Press, 2006.
- Cranmer, K., Brehmer, J., and Louppe, G. The frontier of simulation-based inference. Proceedings of the

- National Academy of Sciences, 2020. doi: 10.1073/pnas.1912789117.
- Dinh, L., Sohl-Dickstein, J., and Bengio, S. Density estimation using real nvp. 2017. URL <https://arxiv.org/abs/1605.08803>.
- Durkan, C., Papamakarios, G., and Murray, I. Sequential neural methods for likelihood-free inference. *arXiv preprint arXiv:1811.08723*, 2018.
- Durkan, C., Bekasov, A., Murray, I., and Papamakarios, G. Neural spline flows. In *Advances in Neural Information Processing Systems*, pp. 7511–7522, 2019.
- Durkan, C., Bekasov, A., Murray, I., and Papamakarios, G. nflows: normalizing flows in PyTorch, November 2020a. URL <https://doi.org/10.5281/zenodo.4296287>.
- Durkan, C., Murray, I., and Papamakarios, G. On contrastive learning for likelihood-free inference. In III, H. D. and Singh, A. (eds.), *Proceedings of the 37th International Conference on Machine Learning*, volume 119 of *Proceedings of Machine Learning Research*, pp. 2771–2781, 2020b.
- Flamary, R. and Courty, N. Pot python optimal transport library, 2017. URL <https://pythonot.github.io/>.
- Greenberg, D., Nonnenmacher, M., and Macke, J. Automatic posterior transformation for likelihood-free inference. In Chaudhuri, K. and Salakhutdinov, R. (eds.), *Proceedings of the 36th International Conference on Machine Learning*, volume 97 of *Proceedings of Machine Learning Research*, pp. 2404–2414, 2019.
- Gutmann, M. U. and Corander, J. Bayesian optimization for likelihood-free inference of simulator-based statistical models. *The Journal of Machine Learning Research*, 17(1):4256–4302, 2016.
- Hermans, J., Begy, V., and Louppe, G. Likelihood-free MCMC with amortized approximate ratio estimators. In III, H. D. and Singh, A. (eds.), *Proceedings of the 37th International Conference on Machine Learning*, volume 119 of *Proceedings of Machine Learning Research*, pp. 4239–4248, 2020.
- Hodgkin, A. L. and Huxley, A. F. A quantitative description of membrane current and its application to conduction and excitation in nerve. *The Journal of physiology*, 117(4):500–544, 1952.
- Kingma, D. P. and Ba, J. Adam: A method for stochastic optimization. *arXiv preprint arXiv:1412.6980*, 2014.
- Kobyzev, I., Prince, S., and Brubaker, M. Normalizing flows: An introduction and review of current methods. *IEEE Transactions on Pattern Analysis and Machine Intelligence*, 2020.
- Lueckmann, J.-M., Goncalves, P. J., Bassetto, G., Öcal, K., Nonnenmacher, M., and Macke, J. H. Flexible statistical inference for mechanistic models of neural dynamics. In *Advances in Neural Information Processing Systems*, pp. 1289–1299, 2017.
- Lueckmann, J.-M., Boelts, J., Greenberg, D. S., Gonçalves, P. J., and Macke, J. H. Benchmarking simulation-based inference. *arXiv preprint arXiv:2101.04653*, 2021.
- Marin, J.-M., Pudlo, P., Robert, C. P., and Ryder, R. J. Approximate bayesian computational methods. *Statistics and Computing*, 22(6):1167–1180, 2012.
- Papamakarios, G. and Murray, I. Fast ε -free inference of simulation models with bayesian conditional density estimation. In *Advances in Neural Information Processing Systems*, pp. 1028–1036, 2016.
- Papamakarios, G., Pavlakou, T., and Murray, I. Masked autoregressive flow for density estimation. In *Advances in Neural Information Processing Systems*, pp. 2338–2347, 2017.
- Papamakarios, G., Nalisnick, E., Rezende, D. J., Mohamed, S., and Lakshminarayanan, B. Normalizing flows for probabilistic modeling and inference. *arXiv preprint arXiv:1912.02762*, 2019a.
- Papamakarios, G., Sterratt, D., and Murray, I. Sequential neural likelihood: Fast likelihood-free inference with autoregressive flows. In Chaudhuri, K. and Sugiyama, M. (eds.), *Proceedings of Machine Learning Research*, volume 89 of *Proceedings of Machine Learning Research*, pp. 837–848. PMLR, 16–18 Apr 2019b. URL <http://proceedings.mlr.press/v89/papamakarios19a.html>.
- Paszke, A., Gross, S., Massa, F., Lerer, A., Bradbury, J., Chanan, G., Killeen, T., Lin, Z., Gimelshein, N., Antiga, L., Desmaison, A., Kopf, A., Yang, E., DeVito, Z., Raison, M., Tejani, A., Chilamkurthy, S., Steiner, B., Fang, L., Bai, J., and Chintala, S. Pytorch: An imperative style, high-performance deep learning library. In Wallach, H., Larochelle, H., Beygelzimer, A., d'Alché-Buc, F., Fox, E., and Garnett, R. (eds.), *Advances in Neural Information Processing Systems 32*, pp. 8024–8035. Curran Associates, Inc., 2019. URL <http://papers.neurips.cc/paper/9015-pytorch-an-imperative-style-high-performance-deep.pdf>.
- Price, L. F., Drovandi, C. C., Lee, A., and Nott, D. J. Bayesian synthetic likelihood. *Journal of Computational and Graphical Statistics*, 27(1):1–11, 2018.
- Radev, S. T., Mertens, U. K., Voss, A., Ardizzone, L., and Köthe, U. Bayesflow: Learning complex stochastic models with invertible neural networks. *IEEE Transactions on Neural Networks and Learning Systems*, 2020.

- Rezende, D. and Mohamed, S. Variational inference with normalizing flows. In International Conference on Machine Learning, pp. 1530–1538. PMLR, 2015.
- Tejero-Cantero, A., Boelts, J., Deistler, M., Lueckmann, J.-M., Durkan, C., Gonçalves, P. J., Greenberg, D. S., and Macke, J. H. sbi: A toolkit for simulation-based inference. Journal of Open Source Software, 5(52): 2505, 2020. doi: 10.21105/joss.02505. URL <https://doi.org/10.21105/joss.02505>.
- Thomas, O., Dutta, R., Corander, J., Kaski, S., and Gutmann, M. U. Likelihood-free inference by ratio estimation. Bayesian Analysis, 2020.
- Wiqvist, S., Mattei, P.-A., Picchini, U., and Frelsen, J. Partially exchangeable networks and architectures for learning summary statistics in approximate Bayesian computation. In Proceedings of the 36th International Conference on Machine Learning. PMLR, 2019.
- Wood, S. N. Statistical inference for noisy nonlinear ecological dynamic systems. Nature, 466(7310):1102–1104, 2010.
- Zaheer, M., Kottur, S., Ravanbakhsh, S., Poczos, B., Salakhutdinov, R. R., and Smola, A. J. Deep sets. In Advances in Neural Information Processing Systems, pp. 3391–3401, 2017.

Supplementary Material to: Sequential Neural Posterior and Likelihood Approximation

Contents – supplementary material

6	Introduction to the supplementary material	11
7	Computer environment	11
8	Performance measures	11
8.1	Kullback–Leibler (KL) divergence	12
8.2	Wasserstein distance	12
8.3	Negative log-posterior of ground-truth parameter	12
9	Incorporating uniform priors in the normalizing flow model for the posterior	12
10	Multivariate Gaussian (MV Gaussian)	12
10.1	Model specification	12
10.2	Computing the KL divergence	13
10.3	Posterior inference	13
11	Complex posterior: Two-moons (TM)	13
11.1	Model specification	13
12	Time-series with summary statistics: Lotka-Volterra (LV)	14
12.1	Model specification	14
12.2	Summary statistics	14
12.3	Dealing with bad simulations	14
12.4	Posterior inference	14
13	Neural model: Hodgkin-Huxley model (HH)	15
13.1	Model specification	15
13.2	Summary statistics	16
13.3	Posterior inference	16
14	Train/validation/test splits	16
15	Hyper-parameter settings	16

6 Introduction to the supplementary material

This document primarily presents additional details on the experimental settings and inference results. However, we also discuss some technicalities on setting up the normalizing flow model for the posterior.

7 Computer environment

The code for replicating the experiments can be found at <https://github.com/SamuelWiqvist/snpla>. All experiments were implemented in `Python 3.7.4`, with normalizing flow models built using the `nflows` package (Durkan et al., 2020a). The `sbi` package (Tejero-Cantero et al., 2020) was used to run SMC-ABC, SNPE-C, SNPR-B, and SNL. We used the `Neuron` software (Carnevale & Hines, 2006) to produce all model simulations for the HH model. Full specifications of the computer environments used are provided in the `env_local.yaml` and `env_lunarc.txt` files. For the multivariate Gaussian (MV Gaussian), two moons (TM), and Lotka-Volterra (LV) we used the LUNARC computer system (<http://www.lunarc.lu.se/>).

8 Performance measures

In this section, we give the definitions of the performance measures used.

8.1 Kullback–Leibler (KL) divergence

The KL divergence for two continuous distributions P and Q is defined as

$$D_{KL}(P|Q) = \int p(x) \log \left(\frac{p(x)}{q(x)} \right) dx,$$

where p and q are the associated probability density functions (pdf). In some cases, the KL divergence is analytically known, and in equation (3) below we give the analytical formula for when P and Q are Gaussian.

8.2 Wasserstein distance

The p^{th} Wasserstein distance between two random variables X and Y on the metric space (M, d) is given by

$$W_p(\mu, \nu) = \left(\inf E[d(X, Y)^p] \right)^{1/p},$$

where d is the distance function on the associated metric space, μ and ν are the marginal distributions of X and Y respectively, and the infimum is taken over all joint distributions of the random variables X and Y with marginals μ and ν . For TM we used the POT: Python Optimal Transport package (Flamary & Courty, 2017) (utilizing the default settings) to estimate the 1st Wasserstein distance based on 1,000 samples from the approximate posterior distributions.

8.3 Negative log-posterior of ground-truth parameter

Assume that we have the posterior approximation $\tilde{p}(\theta|x_{\text{obs}}; \beta_p)$, and the that ground-truth parameter is θ^* . The approximate negative log-pdf of the posterior evaluated at the ground-truth parameter is now given by $\log \tilde{p}(\theta^*|x_{\text{obs}}; \beta_p)$. In our work we compute the negative log-pdf of ground-truth parameter by first approximating $\tilde{p}(\theta|x_{\text{obs}}; \beta_p)$ with a Gaussian distribution, that is estimated from the posterior samples. This step is included to have a consistent approximation of the posterior across models.

9 Incorporating uniform priors in the normalizing flow model for the posterior

The normalizing flow posterior model $\tilde{p}(\theta|x_{\text{obs}}; \beta_p)$ learns the composite transformation $T = T_1 \circ T_2 \circ \dots \circ T_n$ that maps some base distribution u into the parameter posterior distribution $p(\theta|x_{\text{obs}})$. However, if we have a uniform prior for parameter $\theta \sim U(a, b)$, then we know that the posterior will only have non-zero mass on the interval $[a, b]$. This information can be leveraged in the normalizing flow posterior model $\tilde{p}(\theta|x_{\text{obs}}; \beta_p)$ by adding a scaled and shifted sigmoid function $\sigma_{scale, shift}$ as the last transformation in the chain of transformations that constitutes T . Thus, in that case we have that $T = T_1 \circ T_2 \circ \dots \circ T_n \circ \sigma_{scale, shift}$. This way, $\tilde{p}(\theta|x_{\text{obs}}; \beta_p)$ will have positive mass only on the interval $[a, b]$. This is used in all cases where we have uniform priors.

10 Multivariate Gaussian (MV Gaussian)

10.1 Model specification

The conjugate MV Gaussian model of dimension 2 is given by

$$\begin{cases} \mu \sim N(\mu|\mu_\mu, \Sigma_\mu), \\ x \sim N\left(\mu, \Sigma = \begin{bmatrix} 1.3862 & 1.4245 \\ 1.4245 & 1.5986 \end{bmatrix}\right). \end{cases}$$

The hyperparameters μ_μ and Σ_μ are set to

$$\mu_\mu = \begin{bmatrix} 0 \\ 0 \end{bmatrix}, \quad \Sigma_\mu = \begin{bmatrix} 5 & 0 \\ 0 & 5 \end{bmatrix}.$$

Each simulated dataset was generated by first sampling ground-truth parameters for the mean vector μ_{gt} from the corresponding prior distribution. We did this for each of the several versions of the MV Gaussian model.

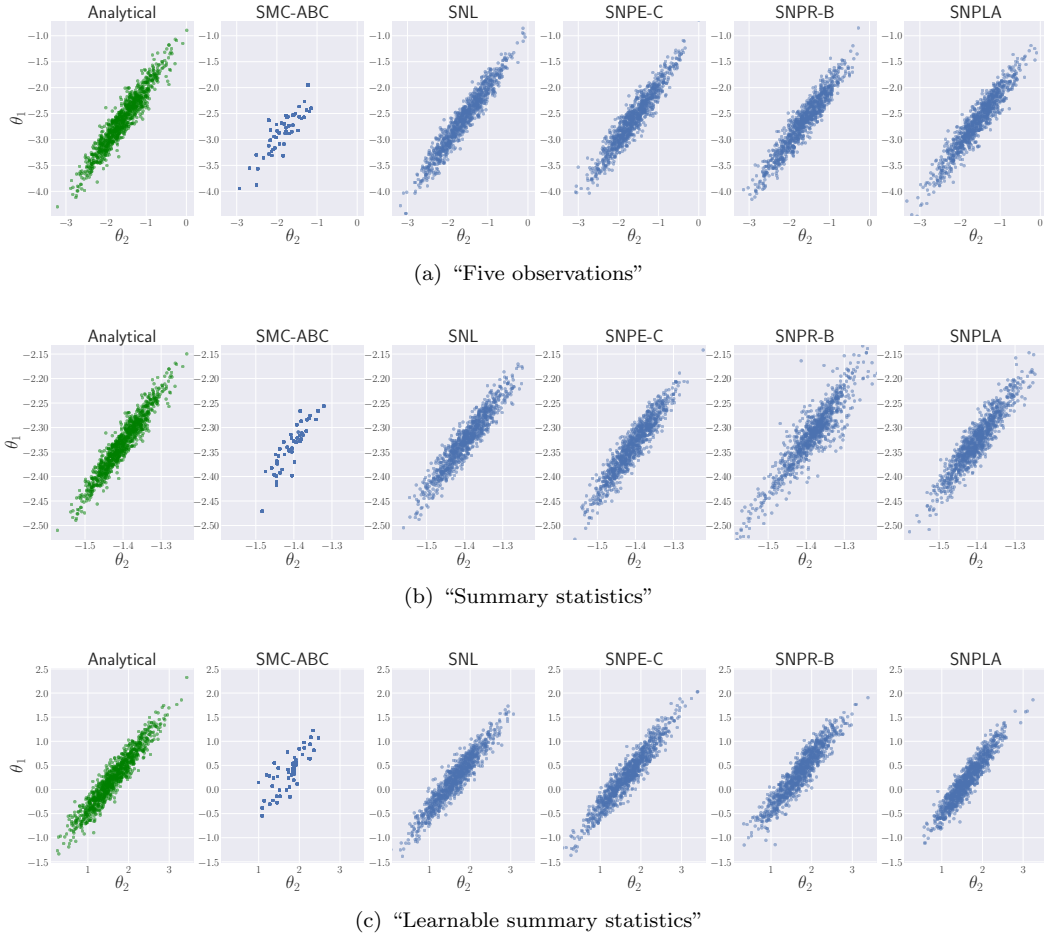


Figure 6: MV:Gaussian: Samples from the resulting posterior approximations for “five observations”, “summary statistics”, and “learnable summary statistics”. Results for one data set.

10.2 Computing the KL divergence

The KL divergence between the analytical posterior $p(\mu|x, \Sigma)$ and some approximation $p^*(\mu|x)$ is given by

$$\begin{aligned}
 D_{KL}(p(\mu|x, \Sigma) || p^*(\mu|x)) &= D_{KL}(N(\mu|m, \Sigma) || p^*(\mu|m^*, \Sigma^*)) \\
 &= \frac{1}{2} \left[\log \frac{\det \Sigma^{*-1}}{\det \Sigma^{-1}} + Tr(\Sigma^{*-1} \Sigma) - D + (m - m^*)^T \Sigma^{*-1} (m - m^*) \right], \quad (3)
 \end{aligned}$$

where m is the mean and Σ the covariance matrix of the analytical posterior. Additionally, m^* and Σ^* are the sample mean and sample covariance matrix based on 1,000 samples from the posterior approximation, respectively. D is the dimension of x , i.e. $D = 2$.

10.3 Posterior inference

Samples from the resulting posterior approximations (for one run) are presented in Figure 6. We conclude that all methods perform similarly well, except for SMC-ABC which performs poorly in all scenarios. Also, for “Summary statistics”, we see that SNRA-B performs considerably worse.

11 Complex posterior: Two-moons (TM)

11.1 Model specification

A full technical description for the TM model can be found in the supplementary material for Greenberg et al. (2019). We followed the model specification in Greenberg et al. (2019), thus we set the observed data to be $x_{\text{obs}} = [0, 0]^T$.

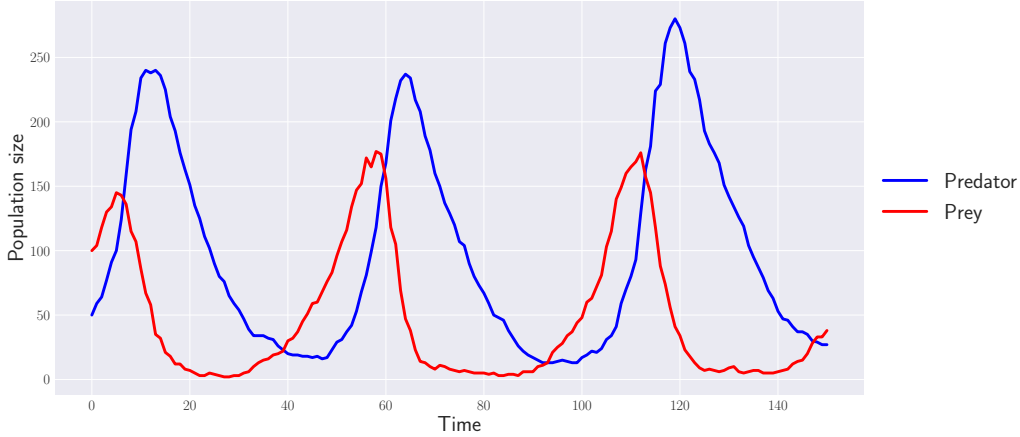


Figure 7: Lotka-Volterra: Simulated data set.

12 Time-series with summary statistics: Lotka-Volterra (LV)

12.1 Model specification

We considered the Markov-jump process version of the LV model presented in the supplementary material of Papamakarios et al. (2019b), including the model specification. The observed data, generated with ground-truth parameters $\theta_{\text{gt}} = [\log 0.01, \log 0.5, \log 1, \log 0.01]^T$, is in Figure 7. For all parameters the prior is uniform on $[-5, 2]$.

12.2 Summary statistics

We used the same nine summary statistics as in Papamakarios et al. (2019b), that is:

- Mean and log variance of each time-series.
- Auto-correlations of each time-series at time lags 1 and 2.
- Cross-correlation between the two time-series.

Before running the inference, a pilot-run procedure was used to make it possible to standardize the summary statistics so that, after standardization, the several components of each summary had a similar relevance. That is, in such a pilot run, we generated 1,000 samples from the prior-predictive distribution: from these summaries, we then computed their trimmed means and trimmed standard deviations (we trimmed the upper and lower 1.25% of the distribution) to eliminate the effect of very extreme outliers. Afterwards, we ran each inference procedure using standardized summaries (both observed and simulated).

12.3 Dealing with bad simulations

Following Papamakarios et al. (2019b) we used the Gillespie algorithm to simulate trajectories from the Lotka-Volterra model. The maximum allowed number of steps to advance the Gillespie simulation, for each given trajectory, was set to 10.000. After 10.000 steps we considered as the output of the simulator at θ the partially simulated trajectory and set to zero the remaining part of the path towards the simulation end-time. Thus, we did not remove parameter proposals that rendered poor simulations.

12.4 Posterior inference

Samples from the resulting posterior approximations for one of the runs are presented in Figure 8. We see that SNL, SNPE-C, and SNRE-B perform similarly well, while SMC-ABC performs much worse. Finally, we conclude that SNPLA (at least for this run) produces a posterior that is more concentrated around the ground-truth parameters. The poor result of SMC-ABC is imputable to its requirement for a much larger set of “particles” (i.e. model simulations).

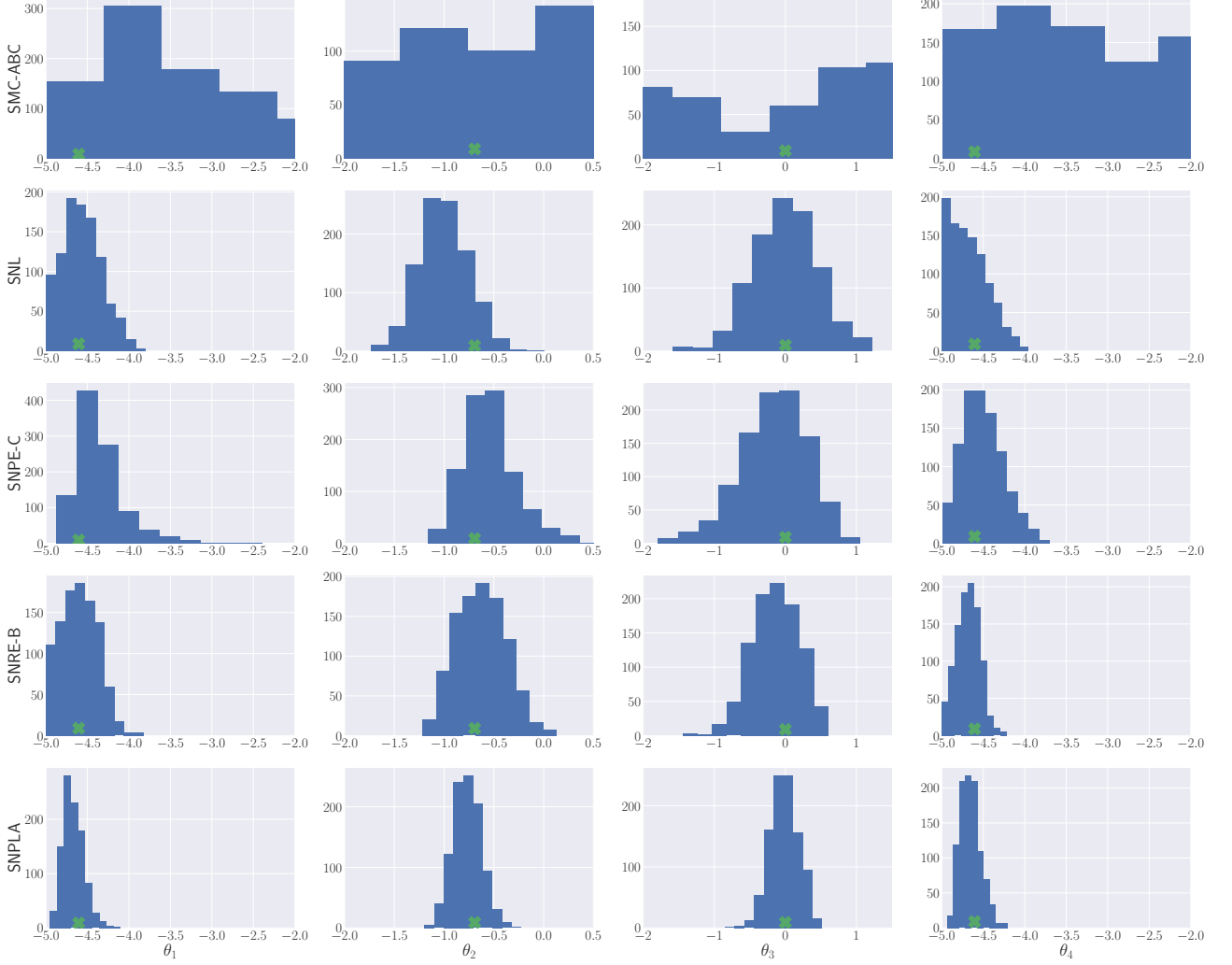


Figure 8: Lotka-Volterra: Samples from the resulting posterior approximations. The green marker shows the true parameter value. Results for one data set.

13 Neural model: Hodgkin-Huxley model (HH)

13.1 Model specification

The HH equations (Hodgkin & Huxley, 1952) model the dynamics of a neuron’s membrane potential as a function of some stimulus (injected current) and a set of parameters. In our experiment, we use the same model formulation as in Lueckmann et al. (2017); Papamakarios et al. (2019b). A full description of the model can be found in the supplementary material for Papamakarios et al. (2019b). Our experimental setting is also similar to Lueckmann et al. (2017); Papamakarios et al. (2019b).

We considered 10 unknown parameters $\theta = [\log(\bar{g}_{Na}), \log(\bar{g}_K), \log(g_{leak}), \log(E_{Na}), \log(-E_K), \log(-E_{leak}), \log(\bar{g}_M), \log(\tau_{max}), \log(V_t), \log(\sigma)]$. The ground-truth values are:

$$\begin{cases} \bar{g}_{Na} = 200 \text{ (s/cm}^2\text{)}, & \bar{g}_K = 50 \text{ (s/cm}^2\text{)}, \\ g_{leak} = 0.1 \text{ (s/cm}^2\text{)}, & E_{Na} = 50 \text{ (mV)}, \\ E_K = -100 \text{ (mV)}, & E_{leak} = -70 \text{ (mV)}, \\ \bar{g}_M = 0.07 \text{ (s/cm}^2\text{)}, & \tau_{max} = 1000 \text{ (mV)}, \\ V_t = 60 \text{ (mV)}, & \sigma = 1 \text{ (uA/cm}^2\text{)}. \end{cases}$$

We followed Papamakarios et al. (2019b) and let the uniform prior for each unknown parameter θ_i be

$$\theta_i \sim U(\theta_i^* - \log(2), \theta_i^* + \log(1.5)), \quad (4)$$

Table 1: Train/validation/test splits for all experiments. R is the number of rounds, N is the number of model simulations per round, N_p the number of total samples from the posterior model used to train SNPLA’s posterior model, valfrac is the fraction of the training data used for validation, $N_{test,post}$ is the number of posterior samples from the posterior approximation at each round, $N_{test,like}$ is the number of sample from the resulting likelihood model (only applicable to SNL and SNPLA).

	R	N	N_p	valfrac	$N_{test,post}$	$N_{test,like}$
MV Gaussian “five observations”	10	2,500	10,000	0.1	1,000	NA
MV Gaussian “summary stats”	10	2,500	10,000	0.1	1,000	1,000
MV Gaussian “learnable summary stats”	10	2,500	10,000	0.1	1,000	NA
Two-moons	5	2,000	40,000	0.1	1,000	1,000
Lotka-Volterra	5	1,000	10,000	0.1	1,000	NA
Hodgkin-Huxley	12	2,000	10,000	0.1	1,000	NA

where θ_i^* is the ground-truth vale for θ_i . We considered C , $\kappa_{\beta n1}$, $\kappa_{\beta n2}$ as known, and these were fixed at

$$C = 1 \text{ (} \mu F/cm^2 \text{)}, \quad \kappa_{\beta n1} = 0.5 \text{ (} ms^{-1} \text{)}, \quad \kappa_{\beta n2} = 40 \text{ (} mV \text{)}.$$

We generated “observed data” from the HH model for 200 ms with a time-step of 0.025 ms . We used the `Neuron` software (Carnevale & Hines, 2006) to produce all model simulations.

13.2 Summary statistics

The likelihood $p(x|\theta)$ was defined on a set of 19 summary statistics that we computed from the voltage time-series produced by the `Neuron` simulator. We used the same 18 summary statistics as in Papamakarios et al. (2019b), and as an additional summary statistic, we included the number of spikes in the voltage time-series. Before running the inference, a pilot-run procedure was used to standardize the summary statistics using a whitening transform. Thus we used a similar standardization scheme for the summary statistics as in Papamakarios et al. (2019b).

13.3 Posterior inference

The posterior samples from SNPE-C, SNL, and SNPLA are in Figures 9, 10, and 11 respectively. We conclude that SNPE-C produces somewhat more informative posterior inference compared to SNL and SNPLA. We also notice that the marginal posteriors are quite similar to the ones reported in Papamakarios et al. (2019b); Lueckmann et al. (2017), except for σ , as in our experiments all compared methods produce worse inference for this parameter.

14 Train/validation/test splits

The train/validation/test splits used for the different experiments are presented in Table 1. Regarding validation data: for SNL, SNPE-C, and SNRE-B, the validation data is set to a fraction valfrac of the training data. Thus, if we use N samples to train the model, $N \times val - frac$ of these samples will be used for validation. This approach of splitting the training and validation data is also used when training the likelihood model for SNPLA. However, a somewhat different approach is used when training SNPLA’s posterior model. Due to the *simulation-on-the-fly* approach, for SNPLA’s posterior model we instead use $N_p \times valfrac$ *additional* simulations for validation purpose.

15 Hyper-parameter settings

The hyper-parameter settings, for all experiments, are in Tables 2-5. Regarding the learn-rate settings: 0.0005 is the default learn-rate used in `sbi`, and 0.001 is the default in the Adam optimizer found in `PyTorch`. We decreased the learn rate for SNPLA’s posterior model using the `PyTorch` function `torch.optim.lr_scheduler.ExponentialLR` with multiplicative factor γ_p , see Table 5 (for details on how the multiplicative factor γ_p is used, see the documentation for `torch.optim.lr_scheduler.ExponentialLR`).

Table 2: SNL: Hyper-parameter-setting for the different experiments for SNL. lr is the learn rate.

	lr
MV Gaussian “five observations”	0.0005
MV Gaussian “summary stats”	0.0005
MV Gaussian “learnable summary stats”	0.0005
Two-moons	0.0005
Lotka-Volterra	0.0005 ^a
Hodgkin-Huxley	0.0005

^aFrom a numerical-stability standpoint we found it for this case to be beneficial to exponential decrease the learn rate with a decay rate of 0.98

Table 3: SNPE-C: Hyper-parameter-setting for the different experiments for SNPE-C. lr is the learn rate.

	lr
MV Gaussian “five observations”	0.0005
MV Gaussian “summary stats”	0.0005
MV Gaussian “learnable summary stats”	0.0005
Two-moons	0.0005
Lotka-Volterra	0.0005
Hodgkin-Huxley	0.0005

Table 4: SNRE-B: Hyper-parameter-setting for the different experiments for SNPE-B. lr is the learn rate.

	lr
MV Gaussian “five observations”	0.0005
MV Gaussian “summary stats”	0.0005
MV Gaussian “learnable summary stats”	0.0005
Two-moons	0.0005
Lotka-Volterra	0.0005
Hodgkin-Huxley	NA

Table 5: SNPLA: Hyper-parameter-setting for the different experiments for SNPLA. lr_L is the learn rate for the likelihood model, lr_P is the learn rate for the posterior model, γ_P is the multiplicative factor of the decrease for the learn rate of the posterior model, and λ is the exponential decrease rate for the prior.

	lr_L	lr_P	γ_P	λ
MV Gaussian “five observations”	0.001	0.002	0.95	0.7
MV Gaussian “summary stats”	0.001	0.002	0.95	0.7
MV Gaussian “learnable summary stats”	0.001	0.002	0.95	0.7
Two-moons	0.001	0.001	0.95	0.8
Lotka-Volterra	0.001	0.001	0.9	0.9
Hodgkin-Huxley	0.001	0.001	0.99	0.7

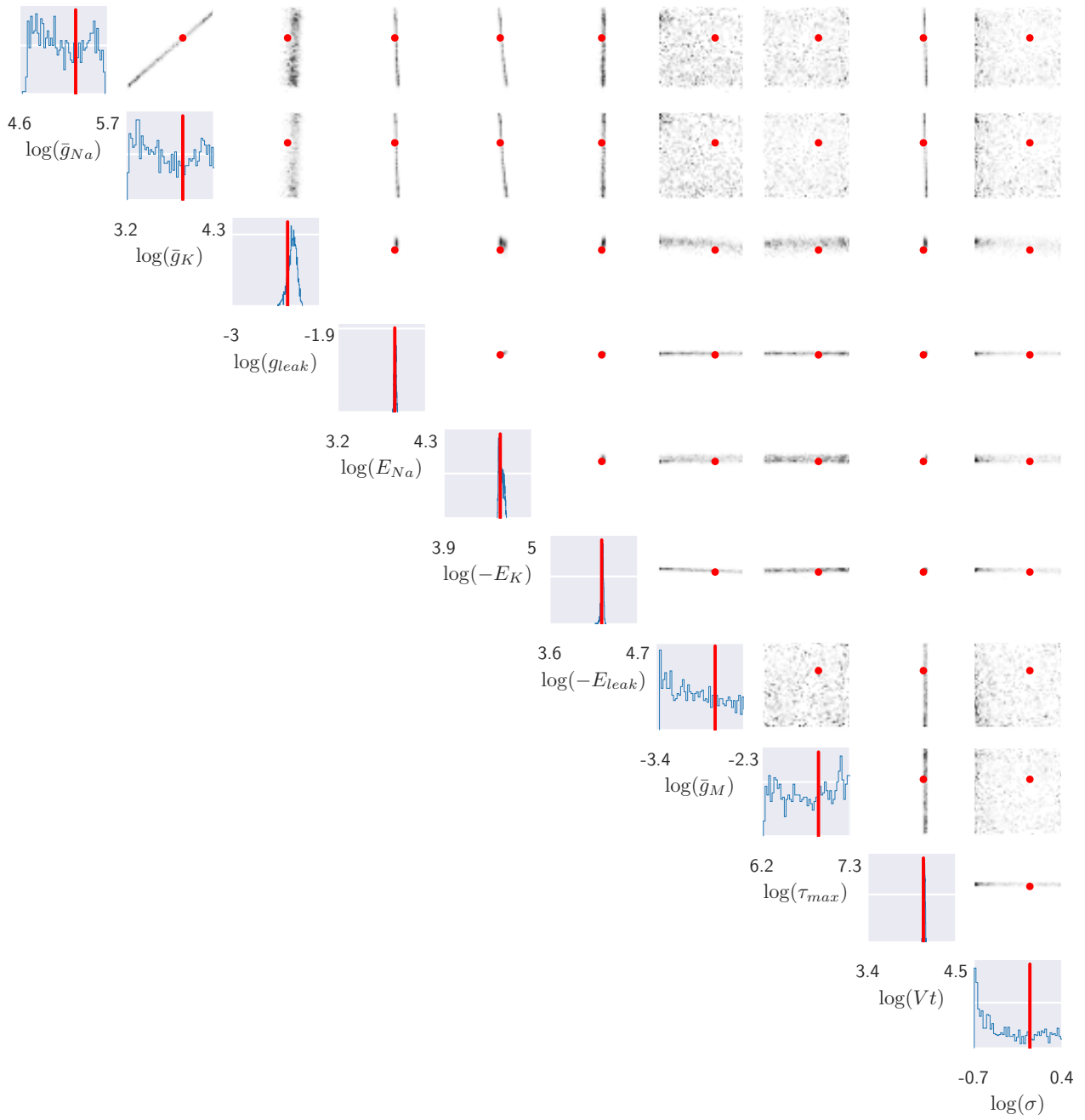


Figure 9: Hodgkin-Huxley: Samples from the posterior approximation for SNPE-C.

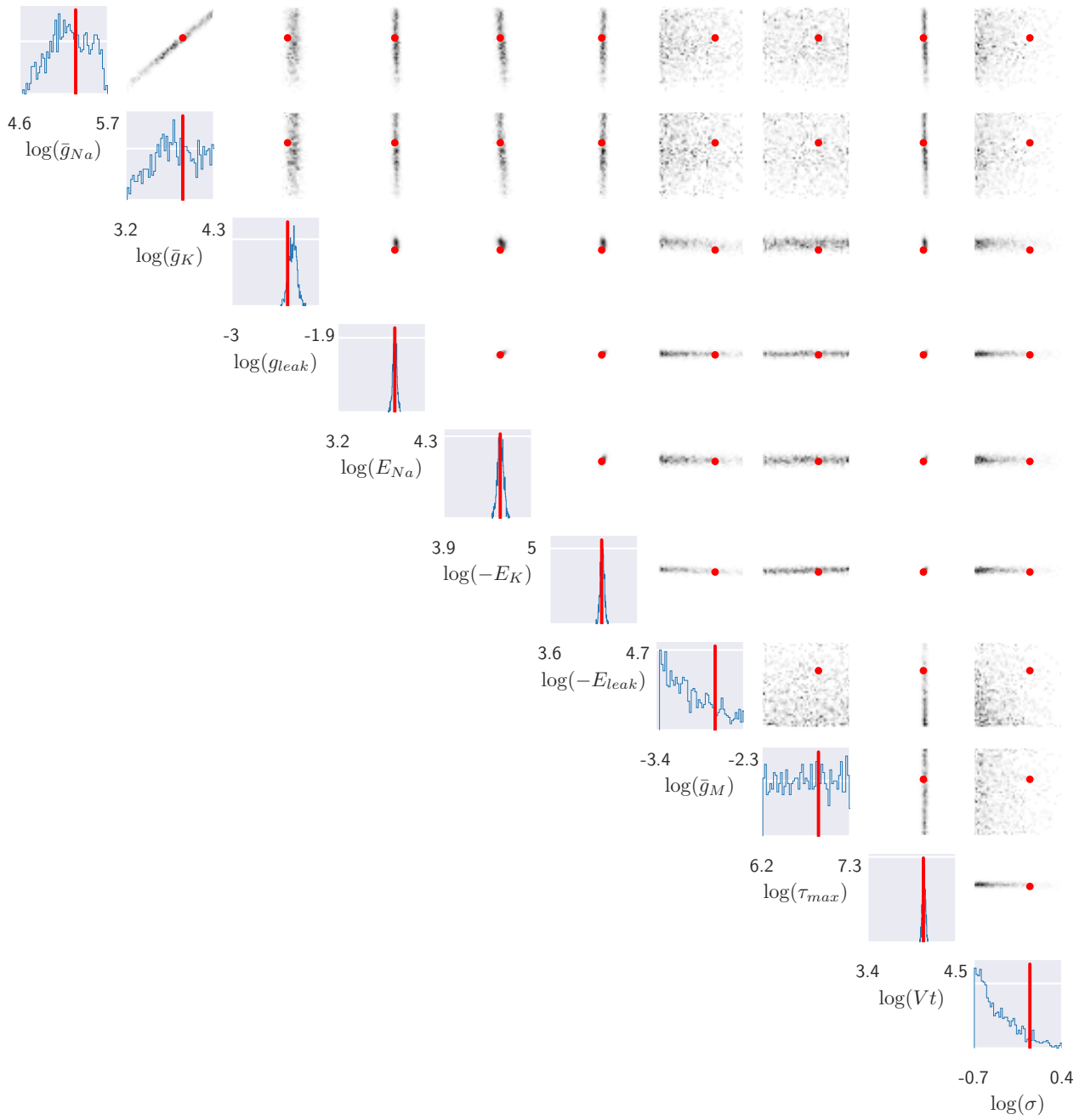


Figure 10: Hodgkin-Huxley: Samples from the posterior approximation for SNL.

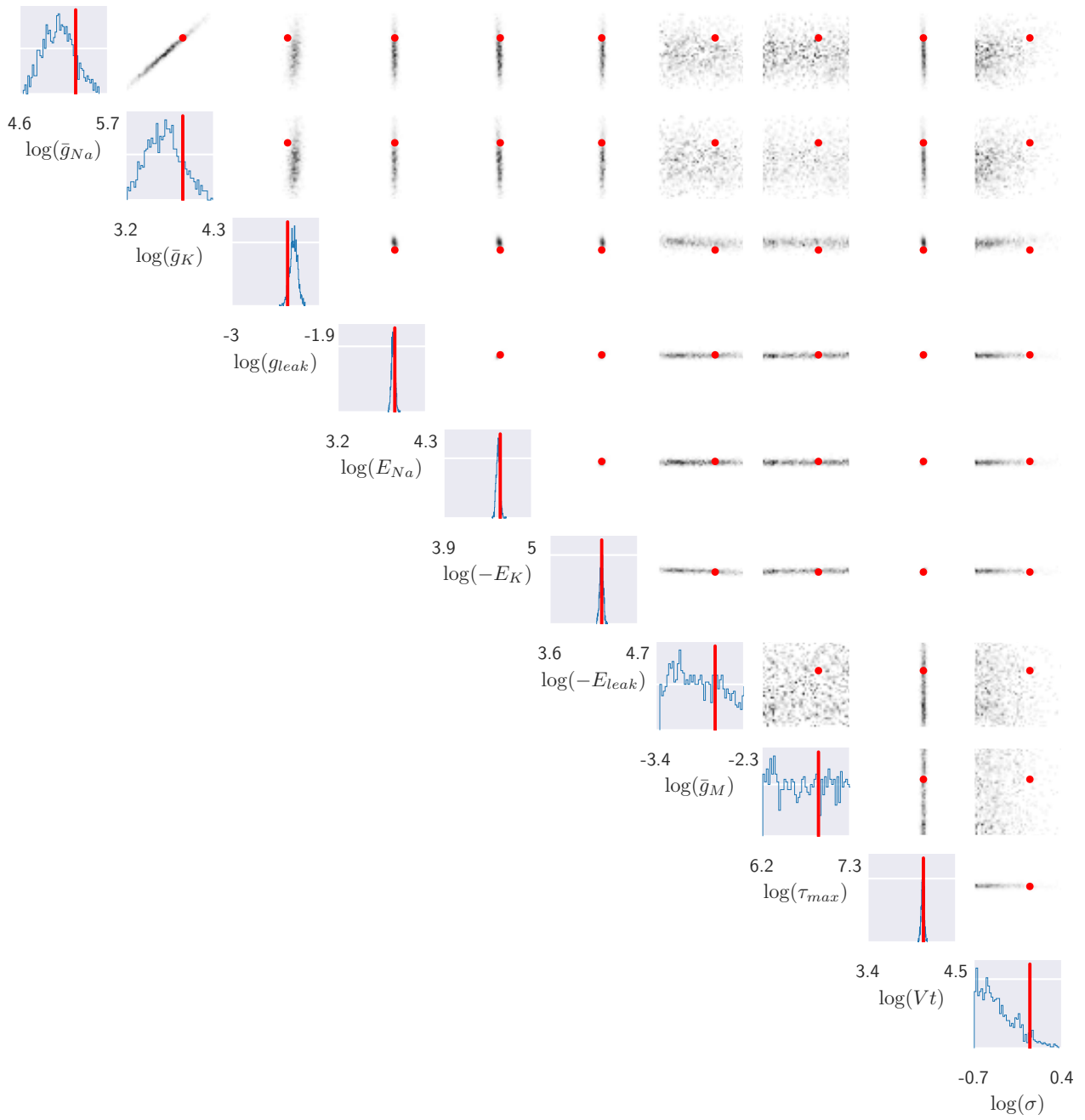


Figure 11: Hodgkin-Huxley: Samples from the posterior approximation for SNPLA.